JOURNAL OF VIROLOGY, Aug. 2004, p. 8271–8280 Vol. 78, No. 15
0022-538X/04/$08.00+0 DOI: 10.1128/JVI.78.15.8271–8280.2004
Copyright © 2004, American Society for Microbiology. All Rights Reserved.

Common E Protein Determinants for Attenuation of Glycosaminoglycan-Binding Variants of Japanese Encephalitis and West Nile Viruses

Eva Lee,[1]* Roy A. Hall,[2] and Mario Lobigs[1]

John Curtin School of Medical Research, Australian National University, Canberra,[1] and Department of Microbiology and Parasitology, University of Queensland, Brisbane,[2] Australia

Received 19 January 2004/Accepted 19 March 2004

Natural isolates and laboratory strains of West Nile virus (WNV) and Japanese encephalitis virus (JEV) were attenuated for neuroinvasiveness in mouse models for flavivirus encephalitis by serial passage in human adenocarcinoma (SW13) cells. The passage variants displayed a small-plaque phenotype, augmented affinity for heparin-Sepharose, and a marked increase in specific infectivity for SW13 cells relative to the respective parental viruses, while the specific infectivity for Vero cells was not altered. Therefore, host cell adaptation of passage variants was most likely a consequence of altered receptor usage for virus attachment-entry with the involvement of cell surface glycosaminoglycans (GAG) in this process. In vivo blood clearance kinetics of the passage variants was markedly faster and viremia was reduced relative to the parental viruses, suggesting that affinity for GAG (ubiquitously present on cell surfaces and extracellular matrices) is a key determinant for the neuroinvasiveness of encephalitic flaviviruses. A difference in pathogenesis between WNV and JEV, which was reflected in more efficient growth in the spleen and liver of the WNV parent and passage variants, accounted for a less pronounced loss of neuroinvasiveness of GAG binding variants of WNV than JEV. Single gain-of-net-positive-charge amino acid changes at E protein residue 49, 138, 306, or 389/390, putatively positioned in two clusters on the virion surface, define molecular determinants for GAG binding and concomitant virulence attenuation that are shared by the JEV serotype flaviviruses.

Japanese encephalitis virus (JEV) and West Nile virus (WNV) are mosquito-borne flaviviruses grouped in the JEV serocomplex, which also includes Murray Valley encephalitis virus (MVE) and St. Louis encephalitis virus (14, 29). Most members of this serocomplex can cause disease in humans, ranging from mild febrile illness to fatal encephalitis. Entry of JEV serotype flaviviruses into mammalian cells is by receptor-mediated endocytosis (reviewed in reference [20]), however, the specific receptor(s) used for virus adsorption and uptake remains elusive.

We and others have shown that flaviviruses have a variable affinity for glycosaminoglycans (GAG) and speculated that this property contributes to the attachment of flaviviruses to host cells (4, 9, 10, 12, 13, 16, 17, 19, 24, 35). GAG are unbranched polysaccharides ubiquitously found on the cell surface and in the extracellular matrix and are usually bound to core proteins (heparan sulfate proteoglycans) (reviewed in reference 2). They are negatively charged due to various degrees of sulfation; accordingly, GAG binding domains typically contain positively charged amino acids. It is most likely that, in addition to attachment of flaviviruses to cell surface GAG, subsequent interaction of attached virus with other host cell receptors is critical for productive virus infection.

Adaptation of flaviviruses to growth in tissue culture cells has been shown to elicit amino acid substitutions that increase the net positive charge of the envelope (E) protein (10, 16, 22, 24). The E protein is the major structural protein that makes up most of the surface of the flavivirus particle and entails a putative receptor-binding domain, numerous neutralization epitopes, and virulence determinants (reviewed in reference 32). Gain-of-positive-charge mutations resulting from host cell adaptation can enhance the ability of flavivirus variants to bind to heparan sulfate proteoglycans and presumably increase the efficiency of virus uptake into a given cell line. However, this selective advantage in growth in tissue culture cells often reduces the virulence of variant viruses in mouse models of flaviviral encephalitis (10, 16, 17, 22, 24). One mechanism for virulence attenuation of GAG binding variants of JEV and MVE prototype strains relative to parent viruses involves their more rapid clearance from the bloodstream by the reticuloendothelial system with the consequence of reducing virus spread and infection of the central nervous system (16).

Virulence attenuation of JEV and MVE as a result of an altered GAG binding phenotype is determined by mutation of one of at least two E protein residues, Glu_{306} and Asp_{390}, respectively (16, 17). Residues 306 and 390 are located in close proximity to each other at the tip of two surface-exposed loops in domain III by analogy with the crystal structure of the tick-borne encephalitis virus and dengue virus E proteins (27, 32). In view of the close genetic and antigenic relatedness of MVE and JEV (81% amino acid identity in the E protein), it is probable that changes at either residue resulting in net gain of E protein positive charge would give comparable virulence attenuation of both viruses. For other members of the JEV serocomplex, attenuated GAG binding variants have not been reported. The aim of this study is (i) to determine the gener-

* Corresponding author. Mailing address: Division of Immunology and Genetics, John Curtin School of Medical Research, Australian National University, P. O. Box 334, Canberra, ACT 2600, Australia. Phone: 61 2 61253526, Fax: 61 2 61252595. E-mail: Eva.Lee@anu.edu.au.

Downloaded from http://jvi.asm.org/ on October 1, 2017 by guest

ality of correlation of gain-of-positive-charge mutations at key E protein determinants, enhanced affinity to cell surface GAG, and reduced virulence for the JEV serotype flaviviruses and (ii) to identify additional E protein residues which can convey the above phenotype.

MATERIALS AND METHODS

Cells and viruses. African green monkey kidney (Vero) cells and human adenocarcinoma (SW13) cells were maintained at 37°C in a humidified atmosphere of 5% CO_2 in minimal essential medium plus nonessential amino acids (Gibco) and 5 or 10% fetal calf serum (Sigma), respectively. Working stocks of WNV strains NY99 (WN-NY99) (15) and MRM61C, an Australian Kunjin virus (KUN) (5), and JEV strains SA14 (JE-SA14/CDC) and FU (JE-FU) (38) were Vero cell supernatants once amplified from original stocks obtained from the Centers for Disease Control, Fort Collins (for JE-SA14 and WN-NY99).

Serial passage of virus in SW13 cells. SW13 cell monolayers in 60-mm dishes (10^6 cells) were infected with virus at a multiplicity of infection of 0.1 Vero PFU/cell, and supernatants were collected and supplemented with HEPES (pH 8.0; 20 mM, final concentration) when significant cytopathic effect was observed. Four subsequent passages were performed for each series with 0.1 ml of the corresponding supernatants and harvesting culture medium each time upon observing significant cytopathic effect. After five passages, plaque-purified stocks were prepared as described before (16) by amplification in SW13 cells.

Sequence analysis. Total cellular RNA from infected SW13 cells (for passage variants) or infected Vero cells (for parent viruses) was extracted with Trizol (Gibco-BRL), precipitated by addition of an equal volume of isopropanol, and washed twice with 70% ethanol. Reverse transcription (RT)-PCR was performed as described before (16) with random hexamers in the RT step and specific primer pairs for PCR: pWN1, 5′-CGG AAT TGC AGT CAT GAT TGG-3′, and pWN2, 5′-AGC CTC CAC ATC ATT GTG TAT-3′ for WN-NY99 and KUN. PCR-amplified cDNA fragments were gel purified and used in cycle sequencing with ABI BigDye v3 chemistry (Applied Biosystems). Additional primers for sequencing of the WNV and KUN M and E genes were 5′-AAC AGA ATC ATG GAT CTT GAG-3′, 5′-GACAGT GGA CTG TGA ACC ACG-3′, 5′-CCA AGG GAG GTT GAG GTC CAT-3′, and 5′-AAG TCC CAA GCT GTG TCT CC-3′. The primers for RT-PCR and sequence analysis of JE-SA14 and JE-FU parent and passage variants have been described (16).

Specific infectivity determination. BHK cells in 60-mm dishes (2×10^6 cells) were infected with parental or SW13 cell-passaged JE-SA14 or JE-Nakayama (16) at a multiplicity of infection of 5 PFU/cell. At 24 h postinfection, the culture supernatant was removed, cells were washed, and fresh medium was added for 2 h before it was harvested and clarified by centrifugation (8,000 × *g*, 5 min at 4°C). The infectivity of virus harvests on Vero and SW13 cells was determined by a 50% tissue culture infectious dose ($TCID_{50}$) assay. Briefly, cells (5×10^3 cells per well) in 96-well plates were infected in multiples of eight with 10-fold serially diluted virus samples (30 μl per well) and incubated for 5 or 6 days, the culture medium was removed, the cell monolayers were fixed in acetone-methanol (1:1), and wells containing virus-infected cells were visualized by enzyme-linked immunosorbent assay (18). $TCID_{50}$ values were calculated by the method of Reed and Muench (31).

Viral RNA in the infected culture supernatant (100 μl) was extracted by the addition of 1 ml Trizol (Gibco-BRL) for 10 min, followed by the addition of 100 μl of chloroform-isoamyl alcohol (24:1; Sigma) and 20 μg of yeast tRNA (Sigma). The aqueous phase was collected after centrifugation (10,000 × *g*, 10 min, 4°C) and mixed with an equal volume of isopropanol, and RNA was pelleted by centrifugation (10,000 × *g*, 15 min, 4°C). RNA pellets were washed twice with 70% ethanol, dried, and resuspended in 20 μl of nuclease-free water (Sigma).

For quantitation of virion RNA content, competitive RT-PCR (8) was performed with a JEV competitor RNA (JE-cRNA) as an internal standard. This was generated by in vitro transcription with T7 RNA polymerase (Promega) of a recombinant pBKS+ (Invitrogen) plasmid containing the JEV-Nakayama genome from nucleotides 564 to 2133 (25), but with an internal deletion from nucleotides 632 to 831. The RNA transcript was incubated at 37°C for 15 min with RNase-free DNase I (Amersham), extracted with Trizol, and precipitated as above; the yield of JE-cRNA from a 25-μl reaction containing 0.1 μg of linear plasmid DNA was routinely 5 to 10 μg. For competitive RT-PCR, the JE-cRNA was serially diluted with nuclease-free water containing 0.5 μg of yeast tRNA/μl; then a series of RNA mixtures containing 1 μl each of diluted JE-cRNA and virion RNA was prepared, initially with 10-fold serially diluted JE-cRNA from 10^{11} to 10^7 copies/ml. RT mix (8 μl) containing antisense primer P1316 (16), Expand reverse transcriptase (Roche), and RNAGuard (Amersham), according to the manufacturer's recommendation, was added to each RNA mixture and incubated at 42°C for 30 min. Reverse-transcribed cDNA (1 μl) was added to a 24-μl PCR mix containing *Taq* DNA polymerase (ABgene) and primers P585, 5′-TGACAA CCA AGA AGT CTA C-3′ and P1316 for JE-SA14, or primers P1316 and P564 (16) for JE-Nakayama, according to the manufacturer's recommendation. The thermal cycling parameters were 94°C for 2 min; 35 cycles of 94°C for 30 s, 55°C for 30 s, and 70°C for 1 min; and 1 cycle of 70°C for 5 min.

PCR products were electrophoresed in 1.2% agarose gels to identify the samples containing two DNA fragments of 770 and 571 bp for JE-Nakayama or 749 and 550 bp for JE-SA14 at similar intensity. The amount of diluted JE-cRNA giving rise to these PCR products allowed quantitation of the virion RNA in the RT mixture, given that the relative yields of DNA fragments derived from virion RNA and JE-cRNA, respectively, reflected the relative molar amounts of the two RNA species in the RT reaction. For more precise quantitation, a second series of RT-PCRs were routinely performed for each virion RNA sample with twofold dilution series of JE-cRNA at concentrations close to the equivalence point.

Heparin-Sepharose binding assay. Heparin-Sepharose and protein A-Sepharose beads (Pharmacia) were suspended in phosphate-buffered saline to 30% (wt/vol) and equilibrated before use by pelleting and washing three times in Hanks' balanced salts solution plus 10 mM HEPES (pH 8.0) and 0.2% bovine serum albumin (HBSS-BSA). Virus (10^5 to 10^6 PFU in 100 μl of HBSS-BSA) and 100 μl of HBSS-BSA with or without Sepharose beads were mixed in Eppendorf tubes and held at 4°C for 6 or 16 h with repeated mixing. Virus mixtures were then centrifuged for 5 min at 6,000 × *g* at 4°C to remove Sepharose beads, and infectious titers in supernatants were determined by plaque assay on Vero cells without further freezing. Two independent experiments were performed for each pair of parental and passaged viruses. Virus samples held in HBSS-BSA for 16 h at 4°C consistently showed 50 to 70% loss of virus infectivity compared with freshly thawed frozen aliquots.

Mouse virulence assay. Swiss out-bred mice 21 to 22 days old were used for virulence assays as described before (22). Briefly, viruses were serially 10-fold diluted in HBSS-BSA, and 30 μl of each dilution inoculated intracerebral or intraperitoneally into groups of five mice. Mortality and morbidity were monitored over 2 weeks.

In vivo virus clearance. Virus (≈10^6 PFU in 100 μl of HBSS-BSA) was inoculated into the tail vein of two weight-matched male 8-week-old BALB/c mice which were anaesthetized with ketamine-xylazol (0.2 ml; 10 mg/ml and 2 mg/ml, respectively). Serum samples were collected over a period of 30 min by periorbital bleeding at specific time points. Virus content in serum was determined by plaque assay on Vero cell monolayers. The inhibitory effects of serum on plaque formation were examined by incubation of ≈100 Vero PFU of each virus stock with normal BALB/c mouse serum diluted 10-, 100-, or 1,000-fold with HBSS-BSA for 15 min at 37°C, followed by titration on Vero cells.

Virus distribution in mouse tissues. Groups ($n = 3$) of 21- to 22-day-old Swiss outbred mice were inoculated intraperitoneally with 500 PFU of WN-NY or WN-NY.P5#1. At 48, 72, or 96 h postinfection, mice were injected with 0.2 ml of ketamine-xylazol, and blood was collected by cardiac puncture, then the brain and spleen were collected after cervical dislocation. Groups ($n = 3$) of 7-week-old male alpha interferon receptor knockout (IFN-α-$R^{-/-}$) mice (21) were inoculated intravenously with 10^3 PFU of KUN parent or KUN.P5#1. At day 3 or 5 (only for KUN.P5#1) postinfection, blood, brain, spleen, and liver were collected as above. The spleen, liver, and brain samples were homogenized as 10% (wt/vol) suspensions in HBSS-BSA, frozen and thawed once, and then clarified by centrifugation for 5 min at 10,000 × *g* at 4°C. Infectious virus contents were determined by plaque assay on Vero cell monolayers.

RESULTS

Adaptation of laboratory strains and natural isolates of WNV and JEV to growth in SW13 cells. To investigate whether host cell adaptation based on altered GAG binding of flaviviruses belonging to the JEV serocomplex is exerted by common structural determinants, we used natural isolates and laboratory strains of WNV (WN-NY99, KUN-MRM61C) and JEV (JE-SA14 and JE-FU) for serial passage in SW13 cells. After 5 passages small plaque variants were plaque-purified and amplified on SW13 cells. The plaque morphology of the SW13 cell-passaged viruses showed a significant reduction in size compared with their corresponding parental strains (Table 1), a property which is characteristic of GAG binding variants and

Downloaded from http://jvi.asm.org/ on October 1, 2017 by guest

TABLE 1. Characteristics of SW13 cell-passaged variants

Virus	Nucleotide changes in E gene[a]	Amino acid changes in E protein[a]	Plaque size[b] (mm)
WN-NY99 parent	NA	NA	5
WN-NY.P5#1	G_{412}→A	Glu_{138}→Lys	<1
WN-NY.P5#2	G_{412}→A	Glu_{138}→Lys	<1
WN-NY.P5#3	G_{412}→A	Glu_{138}→Lys	<1
WN-NY.P5#4	G_{412}→A	Glu_{138}→Lys	<1
KUN parent	NA	NA	5
KUN.P5#1	T_{1119}→C, A_{1169}→G	Silent, Glu_{390}→Gly	2
KUN.P5#2	T_{1119}→C, A_{1169}→G	Silent, Glu_{390}→Gly	2
KUN.P5#3	T_{1119}→C, A_{1169}→G	Silent, Glu_{390}→Gly	2
JE-FU parent			5
JE-FU.P5#1	G_{412}→A	Glu_{138}→Lys	<1
JE-FU.P5#2	G_{412}→A	Glu_{138}→Lys	<1
JE-SA14 parent	NA	NA	5
JE-SA14.P5#1	G_{412}→A	Glu_{138}→Lys	<1
JE-SA14.P5#2	G_{916}→A	Glu_{306}→Lys	<1
JE-SA14.P5#3	G_{145}→A	Glu_{49}→Lys	<1
JE-SA14.P5#4	A_{1166}→G, C_{1146}→T	Asp_{389}→Gly, silent	<1

[a] Parent and passaged variants were sequenced from the start of the M protein gene to the end of the E protein gene. Differences between the passaged variants and the parental viruses are listed. Numbering is from the 5′ and NH_2-terminal residue of the E gene and protein, respectively. KUN parent and passage variants differ from the published sequence (5) as follows: T_{467}→C, resulting in a Phe_{156}→Ser amino acid substitution, which generates a glycosylation site; and C_{858}→G, silent change. JE-FU parent and passage variants differ from the published sequence (38) as follows: silent changes C_{243}→T, T_{267}→C, G_{414}→A, C_{807}→T, and C_{945}→A, as well as C_{323}→T, C_{667}→T, C_{921}→A, C_{923}→T, C_{931}→G, and G_{932}→C resulting in Ser_{108}→Phe, Leu_{223}→Phe, Asn_{307}→Lys, Ser_{308}→Phe, and Arg_{311}→Ala amino acid substitutions, respectively. NA, not applicable.

[b] The plaque sizes of the viruses on neutral-red-stained infected Vero cells were measured at 4 days postinfection.

which is thought to be due to their increased susceptibility to the inhibitory effect of sulfate impurities in the agar overlay.

Specific infectivity of JEV passage variants. The selection of small-plaque variants from JEV and WNV strains serially passaged in SW13 cells suggested a growth advantage of the variants in these cells. To address this directly, the specific infectivity for SW13 and Vero cells based on $TCID_{50}$ value and genome RNA content of JE-SA14 and JE-Nakayama parent and passage variants was compared (Table 2). Js1 was derived from JE-Nakayama by serial passage in SW13 cells (16). To minimise possible infectivity inactivation and contamination by cell debris, the assay was performed on clarified virus-containing culture supernatant collected over a period of 2 h at 24 h postinfection. Infectivity titration of virus stocks by $TCID_{50}$ assay rather than plaque assay was chosen to eliminate a possible influence of sulfate impurities in agar or agarose on infectivity, and the variability in plaquing efficiency of JEV on SW13 cell monolayers. Competitive RT-PCR was performed for quantitation of virion RNA on RNA extracted from the same virus samples used for infectivity determinations. A competitor RNA (JE-cRNA) based on the JE-Nakayama genome and containing an internal deletion was generated by in vitro transcription. Amplification by RT-PCR of mixtures of virion RNA and serially diluted JE-cRNA was performed to generate cDNA products of different sizes, distinguishable in agarose-gel electrophoresis. Use of the JE-cRNA as an internal standard allowed reliable quantitation of as few as 10^3 copies of virion RNA. Both parental strains of JEV showed markedly higher specific infectivity for Vero cells (≤200 genome equiv./$TCID_{50}$) than for SW13 cells (>1.5×10^4 genome equiv./

TABLE 2. Specific infectivity for Vero and SW13 cells of JEV parental and SW13 cell-passaged strains

Virus	Infectivity ($TCID_{50}$/ml)		RNA content (genome equivalents/ml)	Specific infectivity[a]	
	Vero cells	SW-13 cells		Vero cells	SW13 cells
JE-SA14[c]	9.6×10^7	1.2×10^5	3.0×10^9	3.1×10^1	2.5×10^4
	2.0×10^7	2.0×10^5	3.0×10^9	1.5×10^2	1.5×10^4
JE-SA14.P5#1	1.0×10^6	1.0×10^6	6.0×10^8	6.0×10^2	6.0×10^2
JE-SA14.P5#2	1.5×10^6	6.3×10^6	3.0×10^8	2.0×10^2	4.8×10^1
JE-SA14.P5#3[c]	6.8×10^6	1.0×10^7	1.2×10^9	1.8×10^2	1.2×10^2
	1.0×10^7	6.3×10^6	1.2×10^9	1.2×10^2	1.9×10^2
JE-Nakayama	4.0×10^7	3.0×10^4	8.0×10^9	2.0×10^2	2.7×10^5
Js1[b]	2.8×10^6	3.0×10^5	4.0×10^8	1.4×10^2	1.3×10^3

[a] Specific infectivity for Vero and SW13 cells was calculated as the number of virion genome equivalents per $TCID_{50}$.

[b] SW13 cell passage variant derived from JE-Nakayama (16).

[c] Results from two samples are shown.

Downloaded from http://jvi.asm.org/ on October 1, 2017 by guest

$TCID_{50}$), while the passage variants showed comparable specific infectivity for the two cell lines (Table 2). These data are consistent with the view that the relatively poor infectivity of JEV for SW13 cells is a strong selective pressure for the rapid generation of variants with improved growth properties in this cell line.

Genetic changes in the E protein of SW13 cell-adapted variants of WNV and JEV. Sequence analysis was performed on SW13 cell-passaged variants to reveal changes in the viral surface proteins, M and E. Sequencing was on PCR-amplified cDNA derived from total infected cell RNA, with oligonucleotide primers spanning the M and E protein genes. Comparison with the respective parental virus shows that each of the SW13 cell-passaged variants had at least one mutation in the E protein gene (Table 1), while no mutation was found in the M protein gene. Passaged WN-NY99 viruses (4 plaque-purified stocks were analyzed) had a single, identical, nucleotide mutation giving rise to an amino acid change at E protein residue 138 (Glu_{138}→Lys). In KUN-MRM61C-derived passage variants (3 plaque-purified stocks) two nucleotide changes were found: one resulted in an amino acid change at E protein residue 390 (Glu_{390}→Gly), and the second was a silent change. The parental and passaged JE-FU isolates (two plaque-purified stocks) differed at only one nucleotide resulting in an amino acid substitution at E protein residue 138 (Glu_{138}→Lys). Four plaque-purified stocks of SW13 cell-passaged JE-SA14 were sequenced and five different nucleotide changes were found which resulted in amino acid changes at E protein residue 138 (Glu_{138}→Lys) in variant JE-SA14.P5#1, at residue 306 (Glu_{306}→Lys) in JE-SA14.P5#2, at residue 49 (Glu_{49}→Lys) in JE-SA14.P5#3, and at residue 389 (Asp_{389}→Gly) in JE-SA14.P5#4; the last variant also had a silent nucleotide mutation. It is notable that all E protein changes in the SW13 cell-passaged variants resulted in a net acquisition of positive charge (Table 1). There was also repeated occurrence of E protein changes at residues 138 and 390 (analogous to E protein residue 389 in JEV) among the WNV and JEV variants.

Heparin-binding phenotypes of WNV and JEV passage variants. The acquisition of positively charged amino acids in the E protein of SW13 cell-passaged variants of WNV and JEV found in this study in combination with our previous studies on SW13 cell-adapted prototype strains of MVE and JEV (16, 17) suggested enhanced binding of the variants to cell surface GAG as a result of host cell adaptation. This was examined in a binding assay with heparin-Sepharose beads. Virus and beads were incubated in HBSS-BSA with constant mixing and the amount of infectious virus remaining in the supernatant fraction was determined by plaque assays after centrifugation to remove virus bound to the heparin-Sepharose beads. To control for nonspecific loss of virus infectivity and nonspecific binding of virus particles to Sepharose beads, virus was incubated in parallel with HBSS-BSA alone or with similar amounts of protein A-Sepharose beads. Comparison of parental WN-NY99, KUN-MRM61C, JE-FU, and JE-SA14 strains in parallel with their respective passage variants showed poor binding of all parental strains (<23%) in contrast to efficient binding (>96%) of the variants (Fig. 1). It is noteworthy that all six SW13 cell-adapted variants demonstrated comparable binding to heparin-Sepharose not withstanding their genetic

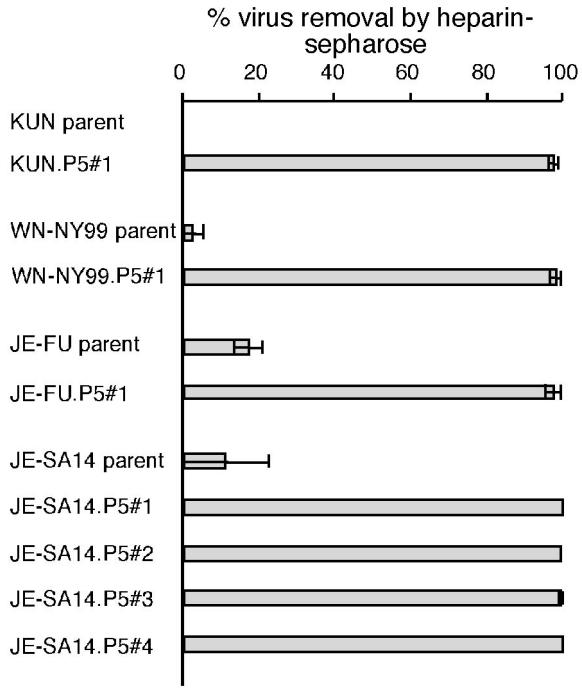

FIG. 1. Clearance of virus with heparin-Sepharose in vitro. Parental and SW13 cell-passaged virus samples were incubated in parallel with HBSS-BSA, heparin-Sepharose beads, or protein A-Sepharose beads. Infectious titers of the unbound virus fractions were determined by plaque assay on Vero cells, and the percentage of virus removed by heparin-Sepharose beads was calculated as (1 − infectious titer of virus mixed with heparin-Sepharose beads/infectious titer of virus mixed with HBSS-BSA) × 100; the standard error of the mean for duplicate samples is shown. The percentage of virus removed by protein A-Sepharose beads was less than 20% for all samples tested.

background and the location of the amino acid changes in the E protein.

Predicted location on the flavivirus E protein of determinants for enhanced GAG binding. Amino acid substitutions associated with enhanced affinity for GAG selected by host cell adaptation of 6 different strains of JEV serocomplex flaviviruses occured at 4 residues in the E protein (this study and references (16, 17). Residues 49, 138, and 389/390 are negatively charged and conserved within the JEV serocomplex but not among other flaviviruses (Fig. 2A).) E protein residue 306, which is altered in one JE-SA14 variant, as well as following SW13 cell passage of the JEV prototype Nakajama strain (16), is either acidic (MVE and JEV) or already basic (WNV and KUN). It is remarkable that the 4 amino acids group into 2 clusters where the pair of residues in each of the clusters are in close spatial proximity when plotted onto the E protein crystal structures of dengue-2 virus (27) and tick-borne encephalitis virus (32) (Fig. 2B). Thus, E protein residues 49 and 138 are located in domain I (on the D0 and E0 beta strands, respectively), and E protein residues 306 and 389/390 are located on the A_xA and FG loops, respectively, residing on the distal lateral face of domain III. The charge property and predicted localization of these key determinants for GAG binding affinity are consistent with a surface-exposed distribution.

Downloaded from http://jvi.asm.org/ on October 1, 2017 by guest

A

```
                49                  138
                ↓                   ↓
JE      VRMINIEAVQLAE   PENIKYEVGIFVH
MVE     I..M....TN..L   ..D......V...
KUN     .K.M.M..AN...   K.......A....
WN      .K.M.M..AN..D   K.......A....
DN2     ELIKTEAKQPATL   P..LE.TIVVTP.
YF      ISLETVAIDRP..   I..LE.TIRAQL.
TBE     .WLDA.YQENP.K   ANK.V.T.KVEP.

                306             389/390
                ↓                   ↓
JE      YGMCTE-KFSFAK   IVVGRGDKQINQH
MVE     ......-..T.S.   ...........H.
KUN     ..V.SK-A.R.LG   ......EQ...H.
WN      ..V.SK-A.K..R   ......EQ...H.
DN2     .S...G-..KVV.   .II.VEPG.LKLN
YF      .KI..D-.MFFV.   .I.....SRLTYQ
TBE     .T..DKT..TWKR   .Y..----ELSHQ
```

B

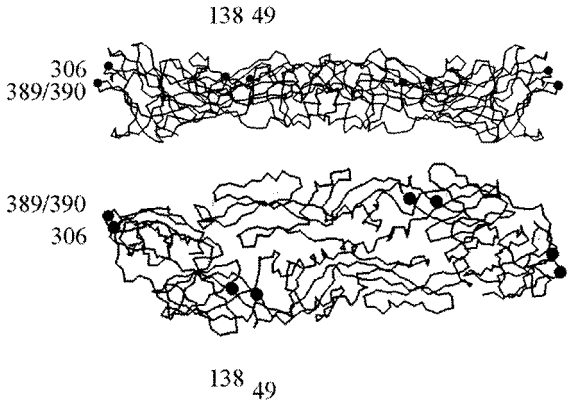

FIG. 2. Location in the flavivirus E protein of key determinants for GAG affinity. (A) E protein sequences of six flaviviruses are aligned to the JE-Nakayama E protein sequence in the regions surrounding residues 49, 138, 306, and 389/390 (JEV and KUN numbering, respectively). Residues identical to those in JE-Nakayama are represented by dots. Sequence information is from references 5, 7, 11, 23, 25, 33, and 37). (B) Location of E protein residues 49, 138, 306, and 389/390 in the crystal structure of the dengue 2 virus E protein ectodomain (27). Side and plane views are shown in the top and bottom panels, respectively. Dots indicate the locations of amino acids which are altered in GAG binding variants of JEV, MVE, and WNV.

Virulence of WNV and JEV GAG binding variants in 3-week-old mice. Adaptation of the prototype strains of JEV and MVE to growth in SW13 cells results in the loss of neuroinvasiveness but not neurovirulence in 3-week-old mice inoculated by the intraperitoneal and intracerebral routes, respectively (16, 22). To investigate the generality among JEV serocomplex flaviviruses of a correlation between host cell adaptation, enhanced GAG affinity, and virulence attenuation, 3-week-old Swiss out-bred mice were infected with parent or passage variants of WN-NY99, KUN-MRM61C, and JE-SA14 viruses with 10-fold decreasing virus doses, titrated on Vero cell monolayers.

The parental KUN-MRM61C strain induced mortality in mice by both intracerebral and intraperitoneal routes of inoculation with 50% lethal doses (LD_{50}) of 0.7 PFU and 0.2 PFU, respectively (Table 3). In contrast, SW13 cell-passaged KUN did not induce mortality by intraperitoneal inoculation even at the maximum dose of 2×10^4 PFU used, despite showing an intracerebral LD_{50} of 5.7 PFU. Given the > 10-fold difference in intraperitoneal/intracerebral LD_{50} ratio, the passage variant is considered attenuated for neuroinvasiveness (28). Parental JE-SA14 induced 100% mortality by either the intraperitoneal or intracerebral routes of inoculation with virus doses greater than 5 PFU. Passage variants JE-SA14.P5#3 and #4 (with E protein changes at residues 49 and 389, respectively) failed to induce mortality following intraperitoneal inoculation of 1.1×10^5 and 5.0×10^4 PFU, respectively. Interestingly, the JE-SA14.P5#3 variant showed partial attenuation of neurovirulence, giving rise to not more than 20% mortality by intracerebral inoculation of up to 10^3 PFU.

TABLE 3. Virulence properties of WNV and JEV passage variants and parental strains

Virus	LD_{50} (PFU on Vero cells)	
	Intracerebral	Intraperitoneal
KUN-MRM61C	0.7	0.2
KUN.P5#1	5.7	$>2 \times 10^4$
WN-NY99	0.06	0.16
WN-NY.P5#1	3.8	38
JE-SA14	<5.5	<5.5
JE-SA14.P5#3	$>1.1 \times 10^3$	$>1.1 \times 10^5$
JE-SA14.P5#4	10	$>5.0 \times 10^4$

WN-NY99 is highly neurovirulent in 3-week-old mice (intracerebral LD_{50} = 0.06 PFU, Table 3). By comparison, the intracerebral LD_{50} value determined for variant WN-NY.P5#1 was > 50-fold higher (3.8 PFU). The intraperitoneal LD_{50} values determined for parental and SW13 cell-passaged WN-NY99 differed by > 200-fold (0.16 and 38 PFU, respectively). Furthermore, a significant difference (P = 0.0028, Mann-Whitney test) was found between WN-NY99 parent and passage variant in average survival times (5.8 ± 0.4 and 8.2 ± 2.6, respectively) of 3-week-old mice inoculated with 10^3 PFU, intraperitoneal.

Virus clearance from the circulation. To examine whether virulence attenuation of GAG binding variants of JEV serocomplex flaviviruses involves the common mechanism of rapid virus clearance from the blood as described for prototype strains of MVE and JEV (16), a high dose of WN-NY99 and KUN-MRM61C parent and variant viruses ($>10^6$ PFU) was administered, intravenously, blood samples collected over 30 min, and infectious virus content measured by plaque-titration on Vero cells (Fig. 3). The parental WN-NY99 strain showed little reduction in virus titers (less than 50%) in the circulation over 30 min whereas the passage variant showed a 3 log drop in virus titers over the same period. A similar trend was observed for parental and SW13 cell-passaged KUN-MRM61C: the parental strain showed a < 10-fold reduction of virus in serum during a 30 min interval in contrast to the > 50-fold reduction found for the passage variant over the same period. Plaque numbers of the four virus stocks tested above were reduced by less than 20% when they were mixed with 1 in 10 diluted mouse serum. Hence, the greater reduction in viremia observed in mice infected with SW13 cell-passaged relative to

Downloaded from http://jvi.asm.org/ on October 1, 2017 by guest

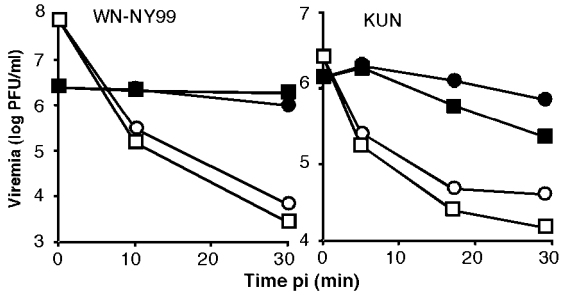

FIG. 3. Virus clearance from the circulation. Parent (solid symbols) and SW13 cell-passaged (open symbols) WN-NY99 and KUN (5×10^6 to 2×10^8 PFU) were inoculated intravenously into two mice each, and virus titers in serum samples collected between 5 and 30 min following injection are shown.

parental viruses was not due to a differential inhibitory effect of mouse serum on virus infectivity.

Tissue distribution of WN-NY99 parent and passage variant in infected 3-week-old mice. The host cell-adapted GAG binding variant derived from WN-NY99 was only marginally attenuated for neuroinvasiveness in the 3-week-old mouse model (intraperitoneal/intracerebral 50% lethal dose [LD_{50}] = 10; see Table 3), in contrast to all other SW13 cell-passaged JEV serotype virus isolates examined so far, which showed a much greater loss of neuroinvasiveness (16, 22; this study). However, consistent with the other SW13 cell-adapted variants, a pronounced increase in the kinetics of blood clearance of variant WN-NY.P5#1 relative to the parent was established. This discrepancy could have been due to the more efficient growth of WNV (in particular viruses with the WN-NY99 genetic background) than JEV and MVE in extraneural tissues of the weanling mice. Thus, attenuation of neuroinvasiveness of the WNV variant in the 3-week-old mouse model could have been concealed by a persistent supply of virus into the circulation from infected extraneural tissues, eventually giving rise to central nervous system infection.

To investigate this proposition, the tissue distribution of parental and variant WN-NY99 following inoculation of 500 PFU intraperitoneally was compared. Swiss outbred mice, 21 to 23 days of age, were used, and virus titers in serum, spleen, and brain collected on days 2, 3, and 4 postinfection from three animals each were determined (Fig. 4). Mice infected with the parental WN-NY99 developed high viremia at 2 days postinfection (3×10^5 to 7×10^5 PFU/ml), declining to $<2 \times 10^3$ PFU/ml on day 4 postinfection. Mean virus titers in spleens were 3×10^5 PFU/g on day 2, rising to 7×10^6 PFU/g on day 4 postinfection. The amount of virus detected in brains collected on days 2 and 3 postinfection was below that of corresponding viremia levels preventing unambiguous determination of the time of neuroinvasion. However, on day 4 postinfection, virus titers in the brains had risen to 10^5 PFU/g and were significantly above viremia levels, clearly showing central nervous system infection.

Viremia detected in mice infected with SW13 cell-passaged WN-NY99 was low (0.6×10^3 to 3.2×10^3) PFU/ml on day 2 postinfection, declining to <200 PFU/ml on day 4 postinfection (Fig. 4), as was expected from the blood clearance data in Fig. 3. Brains collected from mice infected with the passage variant also showed low virus titers ($\approx 10^3$ PFU/g) in one brain harvested on day 3 postinfection and two brains harvested on day 4 postinfection. Notably, the amount of virus in the spleen of mice infected with the WN-NY99 variant (10^5 PFU/g on day 2, 10^6 PFU/g on day 3, and 9×10^5 PFU/g on day 4 postinfection) was not much lower than that found in mice infected with the parent virus. Accordingly, the WN-NY99 GAG binding variant appeared to replicate efficiently in the spleen of weanling mice despite giving rise to low viremia and poor replication in the central nervous system. Replication of the variant in other extraneural tissues was not tested, and the possibility that virus released from such tissues into the circulation contributed to virus detected in the spleen was not addressed.

Virulence and replication of KUN parent and GAG binding variant in type I interferon receptor knockout mice. Our results show high virus titers in the spleen of 3-week-old mice

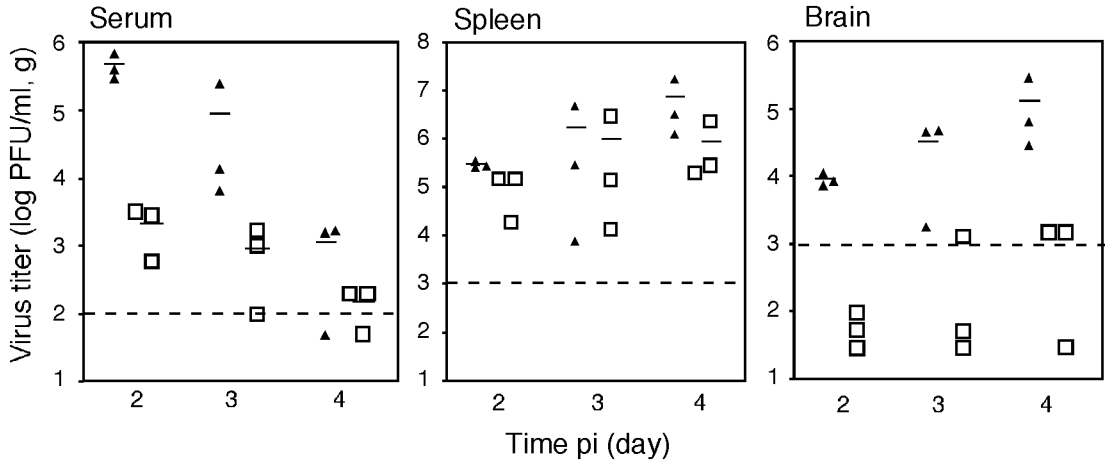

FIG. 4. Virus titers in serum, spleen, and brain of 3-week-old Swiss outbred mice inoculated with parent (solid symbols) or SW13 cell-passaged (open symbols) WN-NY99. Symbols represent titers determined from three individual mice. The lower limit of detection was 10^2 PFU/ml for serum and 10^3 PFU/g for spleen and brain and is indicated by the dashed lines. To calculate mean titers (indicated by horizontal lines), values below the limit of detection were ignored.

Downloaded from http://jvi.asm.org/ on October 1, 2017 by guest

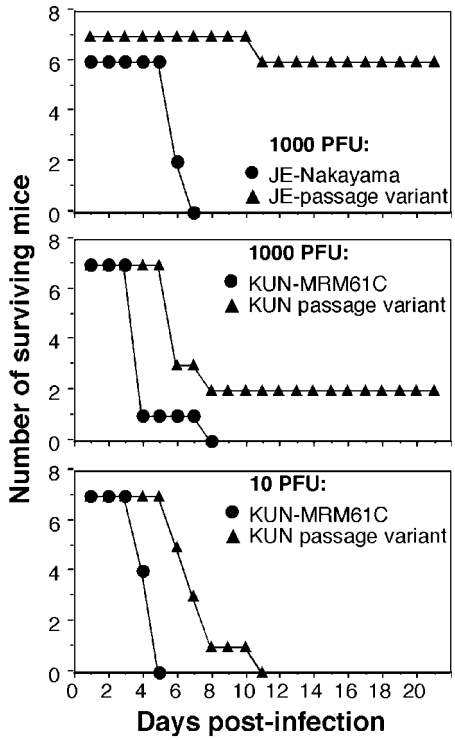

FIG. 5. Susceptibility of IFN-α-R$^{-/-}$ knockout mice to infection with SW13 cell-passaged JE-Nakayama (top panel) and KUN (middle and bottom panels). Seven-week-old mice were used except for the parental JEV virus, which was inoculated into 12-week-old mice. Morbidity and mortality were recorded daily, and surviving mice were monitored for 21 days.

infected with the WN-NY99-derived passage variant, suggesting that infected extraneural tissues can provide a supply of virus into the bloodstream sufficient for neuroinvasion to occur. Next we examined whether a GAG binding variant of KUN also displays a propensity to grow in extraneural tissues, allowing neuroinvasion to occur. KUN has been classified as a low-virulence member of WNV lineage I (1). To increase the sensitivity of detection of virus growth in extraneural tissues, IFN-α receptor knock-out (IFN-α-R$^{-/-}$) mice were used (21).

Groups of IFN-α-R$^{-/-}$ mice (n = 7), 7 weeks of age, were given 10 or 1,000 PFU of KUN parent or passage variant intravenously and observed for 21 days (Fig. 5). IFN-α-R$^{-/-}$ mice were also inoculated intravenously with 1,000 PFU of JE-Nakayama or the corresponding SW13 cell-passaged variant (16). A dose of 10 PFU resulted in 100% mortality for either strain of KUN, whereas the higher dose allowed two of seven mice inoculated with the SW13 cell-passaged KUN to survive while inducing 100% mortality for the KUN parent strain. The time to death of mice infected with the KUN passage variant was delayed in comparison to those infected with the parent virus for both virus doses used (P = 0.03 and 0.0006 for 1,000 PFU and 10 PFU inocula, respectively; Mann-Whitney test). The JEV passage variant was clearly less virulent in IFN-α-R$^{-/-}$ mice than the KUN passage variant. While the JE-Nakayama parent elicited 100% mortality by day 7 postinfection, only one of seven mice infected with the JEV passage variant succumbed at day 11 postinfection.

Virus growth of KUN parent and passage variant in the IFN-α-R$^{-/-}$ mice was examined following inoculation of 10^3 PFU intravenously. Blood, spleen, liver, and brain were collected for the parent virus on day 3 and passage variant on days 3 and 5 postinfection. KUN-infected IFN-α-R$^{-/-}$ mice developed high viremia (1.4×10^9 to 4.6×10^9 PFU/ml) but lower brain titers (4×10^6 to 1.5×10^8 PFU/g) at 3 days postinfection (Table 4); the SW13 cell-passaged KUN elicited 100- to 1,000-fold lower viremia than the parent virus, while brain titers on day 3 postinfection were at or below the limit of detection (Table 4). Notably, virus titers in the spleen of mice infected with the passage variant were comparable to those in parental KUN-infected mice ($>10^8$ PFU/g in each mouse) at 3 days postinfection. The virus titers in the liver of mice infected with the passage variant were ≈10- to 100-fold below those in the liver of parental KUN-infected mice (Table 4). However, the high virus content in serum of parental KUN-infected mice may have contributed to the virus titers in spleen and liver. A similar effect can be excluded for the KUN passage variant, given that viremia were generally lower than the virus titers in the two organs. On day 5 postinfection, mice infected with the variant KUN developed high virus titers in the brain, spleen, and liver, consistent with the observed average survival time of 6.4 days. The very high viremia found in one mouse may have been the result of extensive tissue destruction as a consequence of uncontrolled, fulminant virus growth on day 5 postinfection.

TABLE 4. Growth of parent and GAG-adapted KUN in 7-week-old IFN-α-R$^{-/-}$ mice[a]

Virus	Day	Serum and organ titers (PFU/ml or PFU/g)			
		Serum	Brain	Spleen	Liver
KUN-MRM61C	3	1.4×10^9	4×10^6	4×10^8	4×10^8
		3.8×10^9	6.5×10^6	3×10^8	2×10^8
		4.6×10^9	1.5×10^8	3.5×10^8	1.5×10^8
KUN-P5#1	3	1×10^6	$<10^3$	5×10^8	3×10^6
		5×10^6	$<10^3$	1.3×10^8	1.6×10^7
		3×10^7	4×10^3	5×10^9	3×10^7
	5	2.5×10^{10}	1×10^8	1.6×10^{10}	2×10^9
		1×10^3	7×10^8	2.5×10^{11}	7×10^9
		ND	2×10^7	4×10^{10}	2×10^9

[a] Mice were inoculated intravenously with 10^3 PFU. Virus titers were determined by plaque assay on Vero cells; KUN-P5#1 plaques were uniformly smaller than those of the parent. ND, not determined.

Downloaded from http://jvi.asm.org/ on October 1, 2017 by guest

DISCUSSION

This study defines key residues in the E protein of WNV and JEV for virulence attenuation mediated by a common mechanism of enhanced affinity of the attenuated variants for GAG and, in turn, their reduced ability to disseminate into the central nervous system. With natural isolates and laboratory strains, which differ by as much as 27% in the E protein sequences, we find that host cell adaptation by serial passage in SW13 cells gives rise to a consistent pattern of acquisition of increased net positive charge in E by changes at one of four residues. These residues map to only two clusters by analogy with the E protein crystal structures of tick-borne encephalitis virus and dengue 2 virus: one is defined by E residues 306 and 389/390 and lies at the proximal tip of domain III, and the other is defined by E residues 138 and 49, located on the surface of domain I. The domain III changes at residues 306 and 389/390 were reported by us in previous studies on SW13 cell-passaged prototype strains of MVE and JEV (16, 17, 22), and others have mapped flaviviral molecular determinants for virulence and receptor binding and neutralizing antibody epitopes to the same region in domain III (6, 32). Also consistent with our results, a Glu→Lys substitution at E protein residue 138 has been linked to a small-plaque phenotype and virulence attenuation of JEV isolates NT109 and JaOArS982 (3, 36).

Collectively, these data suggest that all members of the JEV serocomplex can tolerate gain-of-positive-charge changes at E protein residue 49, 138, 306, or 389/390 and that these changes are consistently linked to enhanced GAG binding and reduced virulence. The affinity for heparin was comparable between GAG binding variants altered at any one of the key residues in E. It will be of interest to determine if variants with a combination of changes in the GAG binding sites in E protein domains I and III remain viable and display even greater affinity to heparin or whether the ability to bind heparin plateaus with a single change; the latter would be valuable for stabilization of attenuated phenotypes.

The pattern of E protein changes associated with adaptation of JEV serotype flaviviruses to growth in SW13 cells indicates that variants which interact in a site-specific fashion with GAG were selected. This is distinct from GAG binding variants of tick-borne encephalitis virus selected by serial passage in BHK cells, which resulted in a multitude of single-amino-acid substitutions at residues localized throughout the exposed surface of the E protein (24). In contrast to tick-borne encephalitis virus, serial passage of the Nakayama strain of JEV in BHK cells did not result in any changes in the E protein (our unpublished results). Thus, despite a similar trend towards acquisition of positive charges and enhanced affinity for heparin, it appears that (i) adaptation to BHK and SW13 cells differs fundamentally in the nature and identity of the cellular receptor(s) involved, and (ii) mosquito- and tick-borne flaviviruses utilize a different combination of cellular receptors for attachment and/or entry. It is also notable that JEV passage variants showed increased specific infectivity for SW13 cells but not for Vero cells, suggesting that cell surface GAG plays a lesser role in entry-uptake of JEV into Vero cells compared with SW13 cells.

The present study provides strong evidence for a common mechanism of virulence attenuation of GAG binding variants of encephalitic flaviviruses (Fig. 6). This mechanism entails that, following infection by an extraneural route, dissemination of the variant viruses is inefficient in comparison to the parent viruses due to the enhanced affinity of the variants for GAG found on extracellular matrices and cell surfaces. This was demonstrated experimentally by measuring the in vivo blood clearance kinetics for WNV, JEV, and MVE parent and attenuated strains (16; this study). Importantly, given their efficient removal from the bloodstream, the GAG binding variants often fail to achieve a secondary viremia of sufficient magnitude to allow breach of the blood-brain barrier and establishment of central nervous system infection to occur. Accordingly, the GAG binding variants are poorly neuroinvasive, which is reflected in reduced or absent mortality in 3-week-old mice infected by the intraperitoneal route, as well as low or undetectable secondary viremia.

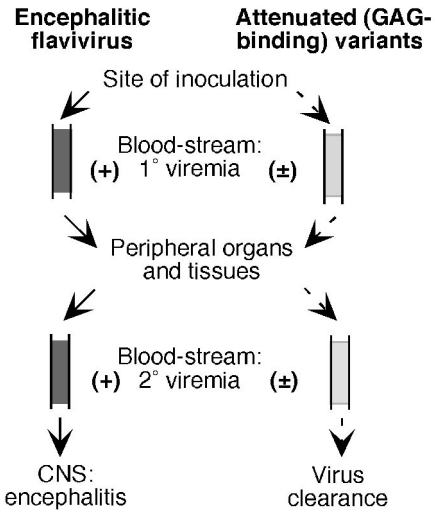

FIG. 6. Schematic model for pathogenesis and virulence attenuation of encephalitic flaviviruses and their GAG binding passage variants. Dashed arrows indicate the processes of replication and dissemination which may be influenced as a result of virus binding to cell surface and extracellular matrix GAG. The reduced level of viremia for GAG binding variants is represented by (±), as opposed to viremia for parental strains (+).

It remains elusive if dissemination of GAG binding variants from extraneural sites of infection is also reduced relative to that of the parental viruses by a mechanism which could involve more efficient reattachment of progeny virus to infected cells. There is evidence in this study that the domain I changes (residues 49 and 138) exert an impact on mouse neurovirulence in addition to that on neuroinvasiveness, on the basis of significantly increased intracerebral LD_{50} values compared with the parental strains. The Glu_{138}→Lys change has been shown by others to reduce the neurovirulence of two strains of JEV, NT109 and JaOArS982 (3, 36). It is notable that the SA14-14-2 live-vaccine strain of JEV, widely used in China, was obtained by extensive laboratory passage in primary hamster and dog kidney cells and differs from the parent SA14 strain in the E protein at residues 138 (Glu_{138}→Lys), 176, 315, and 439 (30). Our serial passage in SW13 cells of the same JE-SA14 strain showed that the Glu_{138}→Lys change, a key

Downloaded from http://jvi.asm.org/ on October 1, 2017 by guest

molecular determinant of virulence attenuation, identifies a GAG binding motif which can be readily acquired during tissue culture adaptation.

Attenuation of neuroinvasiveness of WN-NY99 by passage in SW13 cells was not as dramatic as that of other viruses belonging to the JEV serocomplex according to intraperitoneal and intracerebral LD_{50} determinations in the 3-week-old mouse model. However, heparin-Sepharose affinity and blood clearance kinetics of the WNV variants were comparable to those of JEV, MVE, and KUN variants. Hence, GAG binding variants can differ in their in vivo pathogenicity depending on the genetic background of the parent. The WN-NY99 isolate is similar to the WNV strains that are currently circulating in North America, which have apparently been linked to a greater pathogenic potential in humans and natural hosts as well as in experimental animal models (1, 15, 34). In this respect, it is of interest that virus titers in weanling Swiss outbred mice infected with WN-NY99 showed levels in the spleen significantly higher than those observed in MVE- and JEV-infected mice (16, 26), suggesting a difference in tissue tropism. Moreover, high virus titers were also detected in the spleens of mice infected with the WN-NY99 passage variant, although virus titers in serum and in brain remained low or undetectable. Thus, the most likely explanation for the relatively moderate attenuation of neuroinvasiveness of the WN-NY99 passage variant appears to be the more efficient growth of WNV, relative to JEV and MVE, in extraneural tissues, increasing the supply of progeny virus into the circulation and the probability of central nervous system invasion.

KUN is a naturally attenuated Australian flavivirus and has been classified (on the basis of genotypic relatedness) as belonging to WNV lineage I, a grouping which includes the highly virulent and neuroinvasive American strains of WNV such as WN-NY99 (1). In immunocompetent weanling mice, GAG binding variants of KUN were nonneuroinvasive and indistinguishable in this property from variants derived from JEV and MVE strains. However, with adult mice defective for interferon alpha-beta responses, we found that the KUN passage variant was significantly more virulent than a JE-Nakayama variant (Fig. 5). Furthermore, virus titers in the spleen and liver and possibly other extraneural organs were much higher in KUN than JEV passage variant-infected IFN-α-$R^{-/-}$ mice (Table 4) (16), with the latter showing barely detectable titers in the spleen, liver, and brain on days 2 and 4 postinfection. This finding further supports the notion that WNV and JEV/MVE differ in their ability to grow in extraneural tissues and in the magnitude of subsequent secondary viremia elicited. Accordingly, mutations which enhance GAG binding and, in turn, reduce neuroinvasiveness may be more effective in attenuation of JEV and MVE than WNV for generation of live-vaccine candidates.

ACKNOWLEDGMENTS

This work was supported in part by a grant from the National Health and Medical Research Council of Australia.

We thank Megan Pavy and Debra Nisbet for excellent technical assistance and Alyssa Pike and Greg Smith for facilitating the PC3 animal experiments.

REFERENCES

1. **Beasley, D. W., L. Li, M. T. Suderman, and A. D. Barrett.** 2002. Mouse neuroinvasive phenotype of West Nile virus strains varies depending upon virus genotype. Virology **296:**17–23.
2. **Bernfield, M., M. Gotte, P. W. Park, O. Reizes, M. L. Fitzgerald, J. Lincecum, and M. Zako.** 1999. Functions of cell surface heparan sulfate proteoglycans. Annu. Rev. Biochem. **68:**729–777.
3. **Chen, L. K., Y. L. Lin, C. L. Liao, C. G. Lin, Y. L. Huang, C. T. Yeh, S. C. Lai, J. T. Jan, and C. Chin.** 1996. Generation and characterization of organtropism mutants of Japanese encephalitis virus in vivo and in vitro. Virology **223:**79–88.
4. **Chen, Y., T. Maguire, R. E. Hileman, J. R. Fromm, J. D. Esko, R. J. Linhardt, and R. M. Marks.** 1997. Dengue virus infectivity depends on envelope protein binding to target cell heparan sulfate. Nat. Med. **3:**866–871.
5. **Coia, G., M. D. Parker, G. Speight, M. E. Byrne, and E. G. Westaway.** 1988. Nucleotide and complete amino acid sequences of Kunjin virus: definitive gene order and characteristics of the virus-specified proteins. J. Gen. Virol. **69:**1–21.
6. **Crill, W. D., and J. T. Roehrig.** 2001. Monoclonal antibodies that bind to domain III of dengue virus E glycoprotein are the most efficient blockers of virus adsorption to Vero cells. J. Virol. **75:**7769–7773.
7. **Dalgarno, L., D. W. Trent, J. H. Strauss, and C. M. Rice.** 1986. Partial nucleotide sequence of the Murray Valley encephalitis virus genome. Comparison of the encoded polypeptides with yellow fever virus structural and non-structural proteins. J. Mol. Biol. **187:**309–323.
8. **Gebhardt, A., A. Peters, D. Gerding, and A. Niendorf.** 1994. Rapid quantitation of mRNA species in ethidium bromide-stained gels of competitive RT-PCR products. J. Lipid Res. **35:**976–981.
9. **Germi, R., J. M. Crance, D. Garin, J. Guimet, H. Lortat-Jacob, R. W. Ruigrok, J. P. Zarski, and E. Drouet.** 2002. Heparan sulfate-mediated binding of infectious dengue virus type 2 and yellow fever virus. Virology **292:**162–168.
10. **Goto, A., D. Hayasaka, K. Yoshii, T. Mizutani, H. Kariwa, and I. Takashima.** 2003. A BHK-21 cell culture-adapted tick-borne encephalitis virus mutant is attenuated for neuroinvasiveness. Vaccine **21:**4043–4051.
11. **Gruenberg, A., W. S. Woo, A. Biedrzycka, and P. J. Wright.** 1988. Partial nucleotide sequence and deduced amino acid sequence of the structural proteins of dengue virus type 2, New Guinea C and PUO-218 strains. J. Gen. Virol. **69:**1391–1398.
12. **Hilgard, P., and R. Stockert.** 2000. Heparan sulfate proteoglycans initiate dengue virus infection of hepatocytes. Hepatology **32:**1069–1077.
13. **Kroschewski, H., S. L. Allison, F. X. Heinz, and C. W. Mandl.** 2003. Role of heparan sulfate for attachment and entry of tick-borne encephalitis virus. Virology **308:**92–100.
14. **Kuno, G., G. J. Chang, K. R. Tsuchiya, N. Karabatsos, and C. B. Cropp.** 1998. Phylogeny of the genus *Flavivirus*. J. Virol. **72:**73–83.
15. **Lanciotti, R. S., G. D. Ebel, V. Deubel, A. J. Kerst, S. Murri, R. Meyer, M. Bowen, N. McKinney, W. E. Morrill, M. B. Crabtree, L. D. Kramer, and J. T. Roehrig.** 2002. Complete genome sequences and phylogenetic analysis of West Nile virus strains isolated from the United States, Europe, and the Middle East. Virology **298:**96–105.
16. **Lee, E., and M. Lobigs.** 2002. Mechanism of virulence attenuation of glycosaminoglycan-binding variants of Japanese encephalitis virus and Murray Valley encephalitis virus. J. Virol. **76:**4901–4911.
17. **Lee, E., and M. Lobigs.** 2000. Substitutions at the putative receptor-binding site of an encephalitic flavivirus alter virulence and host cell tropism and reveal a role for glycosaminoglycans in entry. J. Virol. **74:**8867–8875.
18. **Licon Luna, R. M., E. Lee, A. Mullbacher, R. V. Blanden, R. Langman, and M. Lobigs.** 2002. Lack of both Fas ligand and perforin protects from flavivirus-mediated encephalitis in mice. J. Virol. **76:**3202–3211.
19. **Lin, Y. L., H. Y. Lei, Y. S. Lin, T. M. Yeh, S. H. Chen, and H. S. Liu.** 2002. Heparin inhibits dengue-2 virus infection of five human liver cell lines. Antiviral Res. **56:**93–96.
20. **Lindenbach, B. D., and C. M. Rice.** 2001. *Flaviviridae*: the viruses and their replication, p. 991–1041. *In* D. M. Knipe, P. M. Howley, D. E. Griffin, R. A. Lamb, M. A. Martin, B. Roizman, and S. E. Straus (ed.), Fields virology, 4th ed., vol. 1. Lippincott Williams & Wilkins, Philadelphia, Pa.
21. **Lobigs, M., A. Mullbacher, Y. Wang, M. Pavy, and E. Lee.** 2003. Role of type I and type II interferon responses in recovery from infection with an encephalitic flavivirus. J. Gen. Virol. **84:**567–572.
22. **Lobigs, M., R. Usha, A. Nestorowicz, I. D. Marshall, R. C. Weir, and L. Dalgarno.** 1990. Host cell selection of Murray Valley encephalitis virus variants altered at an RGD sequence in the envelope protein and in mouse virulence. Virology **176:**587–595.
23. **Mandl, C. W., F. X. Heinz, and C. Kunz.** 1988. Sequence of the structural proteins of tick-borne encephalitis virus (western subtype) and comparative analysis with other flaviviruses. Virology **166:**197–205.
24. **Mandl, C. W., H. Kroschewski, S. L. Allison, R. Kofler, H. Holzmann, T. Meixner, and F. X. Heinz.** 2001. Adaptation of tick-borne encephalitis virus to BHK-21 cells results in the formation of multiple heparan sulfate binding sites in the envelope protein and attenuation in vivo. J. Virol. **75:**5627–5637.

Downloaded from http://jvi.asm.org/ on October 1, 2017 by guest

25. **McAda, P. C., P. W. Mason, C. S. Schmaljohn, J. M. Dalrymple, T. L. Mason, and M. J. Fournier.** 1987. Partial nucleotide sequence of the Japanese encephalitis virus genome. Virology **158:**348–360.
26. **McMinn, P. C., L. Dalgarno, and R. C. Weir.** 1996. A comparison of the spread of Murray Valley encephalitis viruses of high or low neuroinvasiveness in the tissues of Swiss mice after peripheral inoculation. Virology **220:** 414–423.
27. **Modis, Y., S. Ogata, D. Clements, and S. C. Harrison.** 2003. A ligand-binding pocket in the dengue virus envelope glycoprotein. Proc. Natl. Acad. Sci. USA **100:**6986–6991.
28. **Monath, T. P., C. B. Cropp, G. S. Bowen, G. E. Kemp, C. J. Mitchell, and J. J. Gardner.** 1980. Variation in virulence for mice and rhesus monkeys among St. Louis encephalitis virus strains of different origin. Am. J. Trop. Med. Hyg. **29:**948–962.
29. **Mullbacher, A., M. Lobigs, and E. Lee.** 2003. Immunobiology of mosquito-borne encephalitic flaviviruses. Adv. Virus Res. **60:**87–120.
30. **Ni, H., G. J. Chang, H. Xie, D. W. Trent, and A. D. Barrett.** 1995. Molecular basis of attenuation of neurovirulence of wild-type Japanese encephalitis virus strain SA14. J. Gen. Virol. **76:**409–413.
31. **Reed, L. J., and H. Muench.** 1938. A simple method of estimating 50 per cent endpoints. Am. J. Hyg. **27:**493–497.
32. **Rey, F. A., F. X. Heinz, C. Mandl, C. Kunz, and S. C. Harrison.** 1995. The envelope glycoprotein from tick-borne encephalitis virus at 2 A resolution. Nature **375:**291–298.
33. **Rice, C. M., E. M. Lenches, S. R. Eddy, S. J. Shin, R. L. Sheets, and J. H. Strauss.** 1985. Nucleotide sequence of yellow fever virus: implications for flavivirus gene expression and evolution. Science **229:**726–733.
34. **Roehrig, J. T., M. Layton, P. Smith, G. L. Campbell, R. Nasci, and R. S. Lanciotti.** 2002. The emergence of West Nile virus in North America: ecology, epidemiology, and surveillance. Curr. Top. Microbiol. Immunol. **267:** 223–240.
35. **Su, C. M., C. L. Liao, Y. L. Lee, and Y. L. Lin.** 2001. Highly sulfated forms of heparin sulfate are involved in Japanese encephalitis virus infection. Virology **286:**206–215.
36. **Sumiyoshi, H., G. H. Tignor, and R. E. Shope.** 1995. Characterization of a highly attenuated Japanese encephalitis virus generated from molecularly cloned cDNA. J. Infect. Dis. **171:**1144–1151.
37. **Wengler, G., E. Castle, U. Leidner, and T. Nowak.** 1985. Sequence analysis of the membrane protein V3 of the flavivirus West Nile virus and of its gene. Virology **147:**264–274.
38. **Williams, D. T., L. F. Wang, P. W. Daniels, and J. S. Mackenzie.** 2000. Molecular characterization of the first Australian isolate of Japanese encephalitis virus, the FU strain. J. Gen. Virol. **81:**2471–2480.

Downloaded from http://jvi.asm.org/ on October 1, 2017 by guest